

Influence of Surface Waves on Plasma High Harmonic Generation

Daniel an der Brügge¹, Naveen Kumar¹, Alexander Pukhov¹, Christian Rödel²

¹*Institut für theoretische Physik I, Heinrich-Heine-Universität Düsseldorf, D-40225 Düsseldorf and*

²*Institut für Optik und Quantenelektronik, Friedrich-Schiller-Universität Jena, D-07743 Jena*

The influence of surface plasma waves (SPW) on high harmonic generation (HHG) from the interaction of intense lasers with overdense plasma is analyzed. It is shown, that the surface waves lead to the emission of harmonics away from the optical axis. These off-axis harmonics violate the parity selection rules found from 1D models. Further, our investigations in the highly relativistic regime point towards the existence of a new SPW generation process.

High harmonics generated from solid density plasma surfaces may be about to become the tool that enables the next breakthrough in ultrafast science [1, 2]. Extremely intense XUV attosecond pulses are emitted from plasma surfaces, exploiting the non-linearity of relativistic physics. Because plasmas are used, the process is not subject to the limitations of the methods for generating attosecond pulses in gases [1].

The generation scheme works as follows: an intense laser is incident on a solid surface, immediately ionizing the material. The resulting plasma reflects the light due to its overcritical density. If the field intensity is sufficient, the reflection process becomes strongly non-linear, yielding high harmonics together with the reflected light. Different mechanisms have been identified to be responsible for the high harmonic generation (HHG), some of them already apparent in the sub-relativistic regime, while others take over in the highly relativistic regime [3–5]. All of these theoretical descriptions, including numerical simulations, were formulated in simplified one-dimensional (1D) models, assuming the incoming laser light as well as the reflected radiation to be plane waves [3–6]. Diffraction and focusing of the extremely broadband harmonics radiation in real 3D space can be treated separately, provided the HHG happens “locally independently” at each point in the focal plane [7].

One of the first theoretical results about the surface harmonics have been selection rules concerning the parity and the polarization of the generated radiation [6]. In case of normally incident light, the rule can be derived as follows: The radiation source term is the transverse electron current in the skin layer, $j_y = \rho p_y / \gamma$. Here, $\rho = -e(n_e - n_{e,0})$ is the charge density (ions are assumed immobile), p_y is the transverse momentum component and γ the relativistic γ -factor of the electrons. As the reflected radiation contains the same Fourier components as the source current j_y , we now examine, which Fourier components the individual factors may contain. In the assumed 1D geometry, due to the conservation of canonical momentum, we have $p_y \propto A_y$. Thus, to first order, it oscillates at the laser frequency and we may write $p_y = p_{\text{skin}} e^{-i\omega t}$. Oscillations in the relativistic γ -factor and the charge density ρ on the other hand are determined by the relativistic ponderomotive force and therefore must have a period which corresponds to half of the laser period. They contain only even harmonics,

which we denote by $\rho = \rho_{2\omega}$ and $\gamma = \gamma_{2\omega}$. Consequently, the product $j_y = \rho p_y / \gamma$ contains only odd harmonics, and so does the reflected radiation. In a similar way, selection rules can be derived for oblique incidence, a complete overview of this was given in Tab. 1 of Ref. [6].

The generation of surface plasma waves (SPWs) is a vital feature of laser interaction with overdense plasma. A SPW can propagate long-distances along the surface, while its amplitude falls off exponentially in a direction perpendicular to the surface [8–11]. The dispersion relations of the SPW reads as [11, 12]:

$$ck_{\text{spw}} = \sqrt{\frac{\omega_p^2 - \omega_{\text{spw}}^2}{\omega_p^2 - 2\omega_{\text{spw}}^2}} \omega_{\text{spw}}, \quad (1)$$

where ω_p is the electron plasma frequency, ω_{spw} and k_{spw} are the SPW frequency and wavenumber, respectively. It has been known for some time that a laser impinging on the vacuum overdense plasma surface can generate two counter-propagating SPWs, and this process of SPW excitation was termed the two-surface waves decay (TSWD) process [13–16]. Physically, the ponderomotive force of the laser pulse causes density oscillations at the surface. These density oscillations, at twice of the laser frequency, beat with the electron oscillatory velocity, causing the laser pulse to produce a nonlinear current density which oscillates at one of the SPWs frequencies. For normal incidence of the laser, both SPWs oscillate with the laser frequency itself, forming a standing wave. The SPW becomes parametrically unstable and energy flows into the SPW modes [16]. The expression for the growth rate of the SPWs excitation (cf. Eq. (26) in Ref. [16]) reveals that this process becomes resonant if one chooses initial plasma density to be $\omega_p = 2\omega_0$, where ω_p is the laser frequency. The resonance occurs due to the presence of the dielectric function $\epsilon_{2\omega_0} = 1 - \omega_p^2 / 4\omega_0^2$ in the denominator of the growth rate expression. This resonant excitation of the SPWs in the laser-solid interaction can significantly change the surface morphology. Thus, if present, the SPWs are expected to affect HHG greatly as it occurs from the plasma surface. However, to the best of our knowledge, the influence of SPWs on HHG has never been investigated so far.

In this paper, we study the influence of SPWs on surface HHG on the basis of two sample PIC simulation runs. We thereby focus on normal incidence, as the influence of the SPWs can be pointed out most clearly

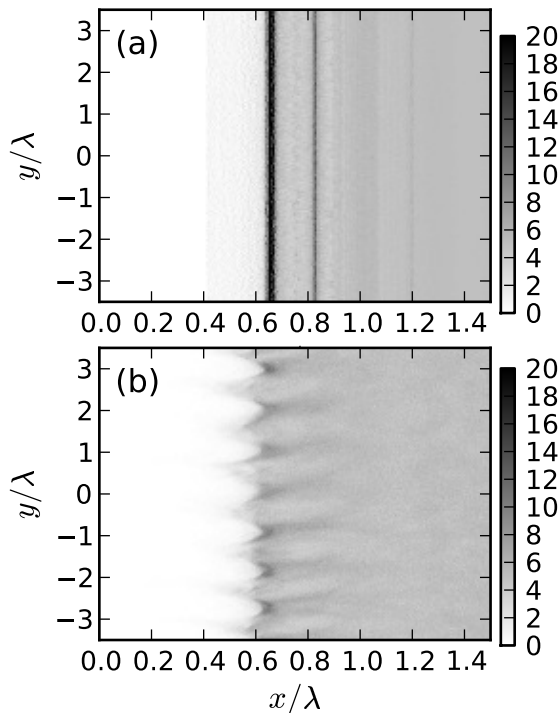


Figure 1: Electron density profile (a) before and (b) after the SPW emerged. Simulation parameters are: $a_0 = 1.7$, $n_{e,0} = 5n_c$. Frame (a) was recorded at simulation time $ct = 4\lambda$, (b) at $ct = 30\lambda$.

here. The first simulation is in the moderately relativistic regime, where we have reason to believe that the analytic description of the TSWD is approximately valid. The second is in the highly relativistic regime, where HHG is supposed to be most efficient and we expect considerable deviation from linear SPW theory.

Let us begin with the first example. For this simulation, we chose parameters similar to the ones in Ref. [14]. The laser is a plane wave, normally incident on the target. Its temporal envelope is given by a linear ramp over three laser periods, up to a constant amplitude of $a_0 \equiv eA/m_e c^2 = 1.7$. The simulation domain is 2D, i.e. all derivatives in z -direction are neglected. Further, the laser \mathbf{E} -field was chosen to point in y -direction. The plasma density leaps from 0 to $n_{e,0} = 5n_c$ within one grid step at $x = 0.5\lambda$. Ions are fixed.

Figure 1 shows the surface density profile at two different times. Frame (a) was recorded at time $ct = 4\lambda$, just after the laser had hit the surface. Here, the electron surface, initially located at $x = 0.5\lambda$, has been pushed in uniformly by about a tenth of the wavelength. Strong variations along the surface are not observed except for some small noise, so at this point the simulation results can still be well described by a 1D model. This changes later in the simulation, as we can see in frame (b), recorded 26 laser cycles later. Here, a SPW has emerged, spontaneously breaking the translational sym-

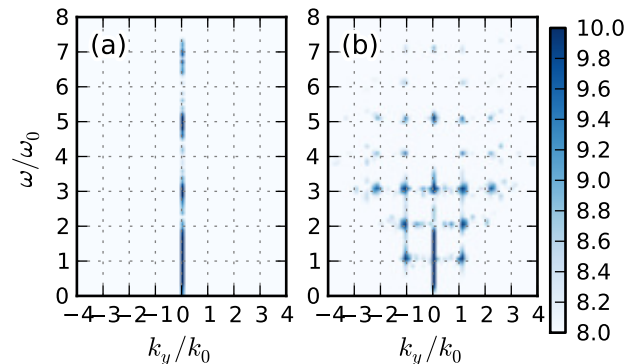


Figure 2: k_y -resolved harmonics spectra, recorded at the left boundary of the simulation box. Simulation parameters are: $a_0 = 1.7$, $n_{e,0} = 5n_c$. Frame (a) corresponds to the time span $ct = 0 \dots 10\lambda$, when the SPW has not yet emerged, and (b) to $ct = 25 \dots 35\lambda$, when the SPW is fully grown. The colour scale corresponds to the logarithm of the spectral intensity, normalization is arbitrary, but consistent.

metry. The wavenumber, measured from the data shown in the figure, is given by $k_{\text{spw}}^{\text{PIC}} \approx 1.1k_0$, very close to what was expected from the linear SPW dispersion relation Eq. (1), $k_{\text{spw}} = 1.15k_0$.

Corresponding spectra of the reflected light are presented in Fig. 2. Again, frame (a) corresponds to an early state, before the SPW builds up. It is seen, that all radiation is reflected at $k_y = 0$, as expected from a plane wave reflected at a smooth surface. We also notice, that harmonics are generated at odd multiples of the laser fundamental, in agreement with the selection rules explained above. Also, we see that all spectral lines are distinctly broadened compared to later times. This can in parts be understood due to the motion of the reflecting surface, especially during the time span, when the laser intensity is still increasing [17]. Frame (b) shows the reflected radiation at the state, where the SPW is fully developed. We see that it possesses a clear signature in the harmonics spectrum. Now, light is not only emitted in specular direction, but also at $k_y = lk_{\text{spw}}$, where l is an integer, numbering the angular sideband. These wavenumbers correspond to angles

$$\vartheta_m^l = \arcsin\left(\frac{lk_{\text{spw}}}{m\omega_0}\right) \quad (2)$$

away from the optical axis, wherein m is the number of the harmonic. Thus, e.g. the 3rd harmonic is measured in specular direction, but also at angles of $\vartheta_3^1 = 22^\circ$ and $\vartheta_3^2 = 47^\circ$ away from the optical axis.

Another remarkable observation is that although the specular light still consists of purely odd-numbered harmonics, the angular sidebands contain both even and odd harmonic numbers. This can be understood with the following perturbative approach. As in the 1D case, the source current is determined by three factors: the charge density ρ , the transverse momentum p_y and

the relativistic factor γ . Assuming that the SPW induces a small perturbation, we neglect its influence on γ , writing $\gamma = \gamma_{2\omega}$ as before. To the factors p_y and ρ , we add a perturbation term representing the SPW: $\rho = \rho_{2\omega} + \delta\rho_{\text{SPW}} \cos(k_{\text{SPW}}y) e^{-i\omega t}$ and $p_y = p_{\text{skin}} e^{-i\omega t} + \delta p_{\text{SPW}} \cos(k_{\text{SPW}}y) e^{-i\omega t}$. Forming the product, we see that

$$j_y = j_y^0 + \cos(k_{\text{SPW}}y) \left(\frac{\delta p_{\text{SPW}} \rho_{2\omega}}{\gamma_{2\omega}} e^{-i\omega t} + \frac{\delta \rho_{\text{SPW}} p_{\text{skin}}}{\gamma_{2\omega}} e^{-2i\omega t} \right) + \mathcal{O}(\delta^2), \quad (3)$$

wherein j_y^0 corresponds to the unperturbed 1D case, thus representing odd harmonics in specular direction. The second summand represents the first angular sideband at $k_y = \pm k_{\text{SPW}}$. Obviously, both even and odd harmonics are contained here. Off-axis even harmonics arise due to the density modulation associated with the SPW, odd ones due to the modulation of the momentum. To assess the higher angular sidebands, terms of the order of δ^2 would have to be taken into account, including the non-linearity of the SPW itself.

Figure 2 contains another important detail. We notice that when the SPW has appeared, the intensity of the higher harmonic orders ($m = 5, 7$) is considerably depleted compared to the 1D case. Thus, it looks as if the TSWD process competes with the HHG process, consuming parts of its energy. This may explain why the HHG with laser pulses in the duration range of 30...100 fs has sometimes fallen behind expectations from 1D models and simulations. For longer pulses, heating of the plasma suppresses the SPWs again.

For the second example, we increase both the laser amplitude and, so as to avoid relativistic transparency, the plasma density. The laser amplitude is raised to $a_0 = 7.2$, the plasma density to $n_{e,0} = 36 n_c$. If we generously extend the resonance condition of the TSWD to allow for excitation at harmonics instead of only the laser fundamental, we write the dielectric term as $\epsilon_{2\omega_m} = 1 - \omega_p^2/4\omega_m^2$, where $\omega_m = m\omega_0$. For our chosen density this term vanishes at $m = 3$, causing a TSWD resonance at the corresponding frequency. Hence for these parameters, the dominant excitation of the SPWs could possibly happen at the third harmonic instead of the fundamental frequency.

Simulation results are presented in Fig. 3. Frame (a) shows the absolute square of the electron density, Fourier transformed in y -direction. This way, SPW modes become immediately recognizable as clearly defined spots in the image. In this example we see that the fundamental does not efficiently excite an SPW, as there is no spot around $k_y = k_0$. This can be expected as the growth rate for the $\omega_{\text{SPW}} = \omega_0$ mode is expected to be very small. Instead, a sharp peak is observed at $k_y^{\text{PIC}} \approx 3.3 k_0$. This value is reasonably close to what is expected from the non-relativistic dispersion relation for $\omega_{\text{SPW}} = 3\omega_0$, which is $k_y = 3.7 k_0$. We therefore conclude that here the 3rd harmonic excites the SPW instead of the laser fundamental. To the best of our knowledge, this excitation process

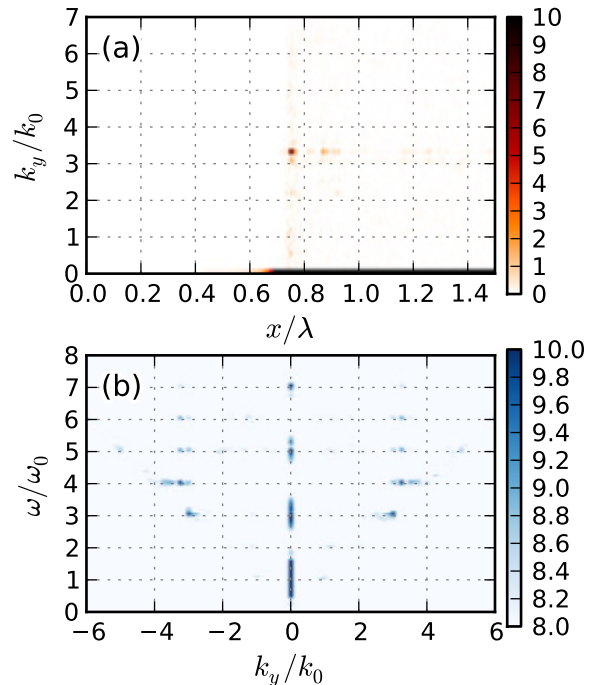


Figure 3: Results of the simulation in the highly relativistic parameter regime: $a_0 = 7.2$, $n_{e,0} = 36 n_c$. Frame (a) shows the absolute square of the Fourier transformed electron density, recorded at $ct = 18\lambda$. The colour scale is linear, units are arbitrary. Frame (b) shows the k_y -resolved electromagnetic spectrum, recorded at the left boundary of the simulation box, during the time window $ct = 10 \dots 25\lambda$. Here, the colour scale is logarithmic.

is completely novel and has not yet been described in the literature. Further simulations carried out by the authors indicate, that this type of excitation process happens frequently in the relativistic regime and is not limited to exact hitting of the assumed resonance. The demonstrated sample however shows a particularly clear case.

As we see from frame (b) of Fig. 3, this process also leaves its footprint in the k_y -resolved spectrum of the reflected field. Here, no sidebands at $k_y = \pm k_0$ or $k_y = \pm 2k_0$ are seen, but one at $k_y = \pm 3k_0$ is clearly observed. As expected, this sideband again contains both even and odd harmonic orders. So e.g. the 4th harmonic order is measured at an angle of $\vartheta_4 \approx 56^\circ$ from the optical axis, but not on the optical axis itself.

Figure 4 shows the growth and damping of the SPW modes in both simulations, represented by an integral over the spatial density spectrum. Frame (a) corresponds to the moderately relativistic simulation. It can be readily seen that after a short period in the beginning ($ct \lesssim 10\lambda$), where both modes grow about equally, the SPW at the fundamental frequency (blue line) grows strongly, whereas other modes are damped. This is expected as we had chosen the plasma density to satisfy

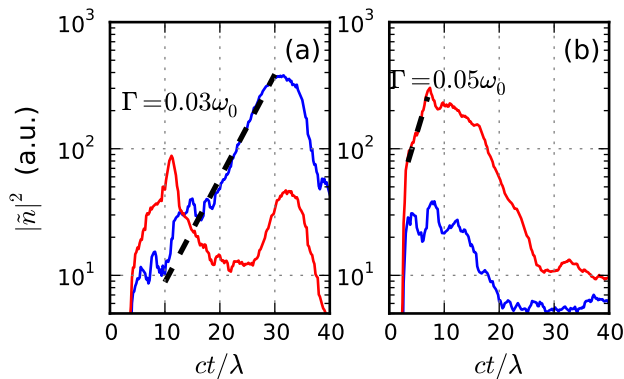


Figure 4: Growth and damping of SPW modes, measured as the spatial spectral intensity of density fluctuations, defined by $|\tilde{n}|^2 \equiv |\int n(x, y, t) \exp(ik_y y) dy|^2$. The blue lines corresponds to modes in the range $0.9 < k_y/k_0 < 1.3$, for this k -range the SPW frequency is roughly ω_0 ; the red lines correspond to $3.0 < k_y/k_0 < 4.0$, so that $\omega_{\text{SPW}} \approx 3\omega_0$. (a) shows results of the moderately relativistic simulation ($a_0 = 1.7$, $n_{e,0} = 5n_c$), (b) of the highly relativistic one ($a_0 = 7.2$, $n_{e,0} = 36n_c$). The black dashed lines show the exponential fits, from which the SPW growth rate has been calculated.

the plasma resonance condition for the generation of two counter-propagating SPWs close to the fundamental laser frequency. After the SPW has reached a certain amplitude, the plasma is heated rapidly and the wave is damped. Results of the highly relativistic simulation are displayed in frame (b). Here, the situation is the other way round: Whereas the SPW at 3rd harmonic can grow quickly, the SPW at fundamental frequency does not reach a high amplitude at all. This can be understood, because with $n_{e,0} = 36n_c$, the density is detuned far from the resonance for the conventional TSWD at the laser fundamental ($n_e = 4n_c$). Consequently, the growth

rate is small and thermal damping sets in, before it can reach a significant amplitude. On the other hand, the 3rd harmonic is exactly at resonance, if one allows for the generous interpretation of the TSWD theory mentioned above. Thus the SPW at this frequency can grow quickly. Note however, that relativistic effects may have a strong bearing on the TSWD process and the SPW dispersion relation. These qualitative discussions are expected to be correct, however quantitative comparisons are difficult to be drawn using the non-relativistic theory. From the PIC simulation, we find the growth rate to be $\Gamma \approx 0.05\omega_0$ within the time range indicated in Fig. 4. Before this stage of linear growth, there is a stage of quasi immediate growth, happening within a fraction of a laser period. After the SPW has reached its peak, it is damped rapidly. Due to its shorter wavelength, this SPW is even more sensitive to thermal damping compared to the SPW at the laser fundamental frequency.

From these results, we deduce that SPW are particularly relevant for laser pulses with the duration in a certain range. If the pulse is too short, the SPW has no time to grow. If the pulse is too long, electron temperature increases and SPWs are damped rapidly. The exact duration depends on the laser and density parameters. In the cases examined here, it was on the range of a few up to a few tens laser periods. Note that this is a duration range, in which many of today's high intensity laser systems work. If SPWs are present, they lead to the production of identifiable angular sidebands in the harmonics radiation. The angles of the sidebands can be estimated by Eq. (2). As the k_y -components of the sidebands are constant, the angles are greater for lower harmonic orders in the optical range and smaller for high orders.

This work was supported by DFG in the framework of the TR 18 project.

-
- [1] G. D. Tsakiris, K. Eidmann, J. Meyer-ter-Vehn, and F. Krausz, *New Journal of Physics* **8**, 19 (2006).
 - [2] F. Krausz, *Reviews of Modern Physics* **81**, 163 (2009).
 - [3] T. Baeva, S. Gordienko, and A. Pukhov, *Phys. Rev. E* **74**, 046404 (2006).
 - [4] D. a. d. Brügge and A. Pukhov, *Physics of Plasmas* **17**, 033110 (2010).
 - [5] C. Thaury and F. Quéré, *Journal of Physics B: Atomic, Molecular and Optical Physics* **43**, 213001 (2010).
 - [6] R. Lichters, J. Meyer-ter-Vehn, and A. Pukhov, *Phys. Plasmas* **3**, 3425 (1996).
 - [7] D. a. d. Brügge and A. Pukhov, *Physics of Plasmas* **14**, 093104 (2007).
 - [8] P. K. Kaw, *Physics of Fluids* **13**, 1784 (1970).
 - [9] V. M. Agranovich, *Soviet Physics Uspekhi* **18**, 99 (1975).
 - [10] H. Lee and S. Cho, *Physical Review E* **59**, 3503 (1999).
 - [11] J. M. Pitarke, V. M. Silkin, E. V. Chulkov, and P. M. Echenique, *Reports on Progress in Physics* **70**, 1 (2007).
 - [12] L. Landau, E. M. Lifshitz, and L. P. Pitaevskii, *Electrodynamics of continuous media* (Elsevier/Butterworth Heinemann, Amsterdam [etc.], 2008), 2nd ed., ISBN 9780750626347.
 - [13] K. Yasumoto and T. Noguchi, *Journal of Applied Physics* **53**, 208 (1982).
 - [14] A. Macchi, F. Cornolti, F. Pegoraro, T. Liseikina, H. Ruhl, and V. Vshivkov, *Physical Review Letters* **87** (2001).
 - [15] A. Macchi, F. Cornolti, and F. Pegoraro, *Physics of Plasmas* **9**, 1704 (2002).
 - [16] N. Kumar and V. K. Tripathi, *Physics of Plasmas* **14**, 103108 (2007).
 - [17] M. Behmke, D. an der Brügge, C. Rödel, M. Cerchez, D. Hemmers, M. Heyer, O. Jäckel, M. Kübel, G. Paulus, G. Pretzler, et al., *Physical Review Letters* **106** (2011).